Loss of SUMO1 in mice affects RanGAP1 localization and formation of PML nuclear bodies, but is not lethal as it can be compensated by SUMO2 or SUMO3

Evgenij Evdokimov[1], Prashant Sharma[1], Stephen J. Lockett[2], Margaret Lualdi[3] and Michael R. Kuehn[1,*]

[1]Laboratory of Protein Dynamics and Signaling, National Cancer Institute, National Institutes of Health, NCI-Frederick, Frederick, MD 21702, USA
[2]Optical Microscopy and Analysis Laboratory, Advanced Technology Program, SAIC-Frederick, Frederick, MD 21702, USA
[3]Laboratory Animal Sciences Program, SAIC-Frederick, Frederick, MD 21702, USA
*Author for correspondence (e-mail: mkuehn@mail.nih.gov)

Accepted 16 September 2008
Journal of Cell Science 121, 4106-4113 Published by The Company of Biologists 2008
doi:10.1242/jcs.038570

Summary

Conjugation of the small ubiquitin-like modifier (SUMO) to target proteins regulates numerous biological processes and has been implicated in tumorigenesis and metastasis. The three SUMO isoforms in vertebrates, SUMO1 and the highly similar SUMO2 and SUMO3, can be conjugated to unique as well as overlapping subsets of target proteins. Yet, it is still not clear whether roles for each family member are distinct or whether redundancy exists. Here we describe a mutant mouse line that completely lacks SUMO1, but surprisingly is viable and lacks any overt phenotype. Our study points to compensatory utilization of SUMO2 and/or SUMO3 for sumoylation of SUMO1 targets. The ability of SUMO isoforms to substitute for one another has important implications for rational targeting of the SUMO pathway.

Supplementary material available online at
http://jcs.biologists.org/cgi/content/full/121/24/4106/DC1

Key words: SUMO, RanGAP1, PML

Introduction

The capacity for members of the structurally related ubiquitin-like (Ubl) family, including SUMO, to profoundly influence the stability, subcellular localization and activity of proteins to which they are covalently conjugated is now well established (Kerscher et al., 2006). Modification of proteins with SUMO, or sumoylation, regulates many essential cellular activities, including nucleocytoplasmic transport, transcription, and maintenance of genome integrity (Geiss-Friedlander and Melchior, 2007; Gill, 2004; Girdwood et al., 2004; Hay, 2005; Johnson, 2004), and has been implicated in tumorigenesis and metastasis (Baek, 2006; Seeler et al., 2007). A large number of proteins have now been shown to be sumoylated, with the outcome varying depending on the target protein. For example, sumoylation of the RanGTPase-activating protein, RanGAP1, regulates its localization to the nuclear pore (Matunis et al., 1996; Muller et al., 1998). Conjugation to the promyelocytic leukemia protein PML, as well as noncovalent SUMO binding, promotes higher-order assembly of discrete nuclear bodies and the recruitment of other sumoylated proteins to these structures (Lin et al., 2006; Shen et al., 2006; Sternsdorf et al., 1997).

There are three functional SUMO isoforms in higher eukaryotes; the almost identical SUMO2 and SUMO3 (here referred to as SUMO2/3) and the more distantly related SUMO1. Covalent attachment of these different SUMO isoforms to target proteins is achieved by the same conjugation pathway, which is mechanistically similar to that of other ubiquitin-like proteins. Sequential activities including the E1-activating enzyme, a single E2-conjugating enzyme, Ubc9 and various E3-specificity factors, promote attachment of SUMO to lysine residues, often within a specific consensus sequence. Sumoylation is a reversible dynamic process, with deconjugation mediated by SUMO proteases (SENP/SUSPs). These vary in subcellular localization and show preferential activity against substrates conjugated with specific SUMO isoforms (Mukhopadhyay and Dasso, 2007; Yamaguchi et al., 2005). Proteomic studies have shown that SUMO1 and SUMO2/3 can be conjugated to unique target subsets but also show some overlap in target specificity (Rosas-Acosta et al., 2005; Vertegaal et al., 2006; Vertegaal et al., 2004). Other studies have revealed differences in the behavior and dynamics of SUMO isoforms (Ayaydin and Dasso, 2004; Fu et al., 2005; Mukhopadhyay and Dasso, 2007; Saitoh and Hinchey, 2000; Tatham et al., 2005; Zhang et al., 2008). Together, these data suggest distinct functions for SUMO1 compared with SUMO2/3. However, there is still no clear understanding of which roles are unique and to what degree any redundancy exists.

To begin to uncover exclusive versus shared functions for SUMO isoforms we have derived mutant mice completely lacking SUMO1. Here we show that SUMO1 mutants are viable and without any overt phenotype, although mutant cells do have reduced localization of RanGAP1 at the nuclear pore and significantly fewer PML nuclear bodies. We demonstrate compensatory utilization of SUMO2/3 for RanGAP1, suggesting redundancy is an important cellular strategy for maintaining sumoylation levels above critical thresholds.

Results

Derivation of SUMO1 mutant mice from XA024 gene trap ES cells

To generate mice lacking SUMO1, we utilized a gene trap ES cell line from the BayGenomics resource (Stryke et al., 2003). In the XA024 line, the *SUMO1* locus is disrupted by insertion of a gene trap vector into the first intron. Animals derived from this cell line and heterozygous for the insertion, identified initially by the presence of the β-geo allele carried by the gene trap vector (Fig. 1), were normal. To analyze homozygotes, we first determined the

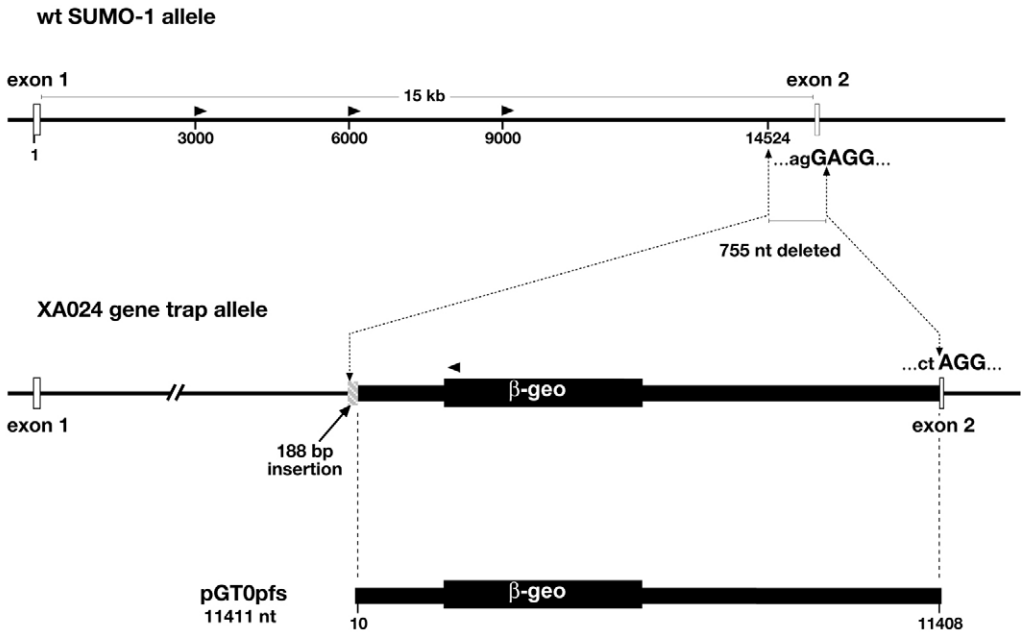

Fig. 1. Structure of the XA024 gene-trap insertion. Upper, schematic representation of exon 1, intron 1 and exon 2, of the wild-type *SUMO1* gene showing the positions of forward primers (arrowheads) used for long-range PCR to localize the insertion. The sequence at the junction between intron 1 and exon 2 is shown (intron in small and exon in capital letters). The position of the insertion and the region of intron 1 deleted in the gene-trap allele are indicated. Middle, structure of the gene trap allele showing inserted vector and reverse primer used for long range PCR. The sequence at the junction of the inserted vector and exon 2 is shown (gene trap vector in small and exon in capital letters); the first nucleotide of exon 2 is lost. Lower, structure of the gene trap vector; the majority was retained in the insertion event.

exact point of integration of the gene trap vector to provide sequence information necessary for unambiguous PCR-based genotyping. To localize the vector insertion site, we carried out long-range PCR using primers located at various points along the length of the 15 kb first intron with an anchor primer at the 5′ end of the vector. This allowed us to establish that insertion of the vector occurred at the very 3′ end of the first intron and resulted in deletion of the final 754 intronic nucleotides as well as the first nucleotide of exon 2 (Fig. 1). Owing to loss of the splice acceptor sequences, exon 2 is in effect now part of a fused exon with the gene trap vector. This is an unusual structure for gene trap insertions, which are normally found wholly within introns, and suggested that this allele should be severely affected.

XA024 SUMO1 gene trap homozygotes are phenotypically normal

To determine the consequences of homozygosity for the disrupted *SUMO1* allele, we mated heterozygous animals and either let litters go to term or collected embryos at various prenatal stages. For genotyping, we used PCR primers from within exon 2, along with primers from either the 3′ end of the vector or 3′ end of intron 1 to distinguish the gene-trap and wild-type alleles, respectively (Fig. 1). We identified homozygous embryos at various developmental stages (supplementary material Fig. S1) as well as homozygous live-born pups, none of which showed any overt phenotypic defects. Overall, an examination of almost 200 fetuses and 100 mice derived from heterozygous crosses showed no deviation from mendelian expectations and no abnormalities. In addition, homozygous adults were fully fertile and offspring from homozygous intercrosses were completely normal. These data suggested that SUMO1 is dispensable.

Complete loss of SUMO1 in XA024 mice

The above results were unexpected given the recent report on mice derived from a different SUMO1 gene-trap line, RRQ016. Homozygotes were reported to die at pre- and perinatal stages, with heterozygotes manifesting craniofacial defects (Alkuraya et al., 2006). To confirm that integration of the vector in XA024 indeed disrupts *SUMO1* expression we first carried out RT-PCR analysis on wild-type, heterozygous and homozygous embryonic mRNA samples, using primers specific for exons on either side of the insertion as well as within the vector (Fig. 2A). We found the expected spliced transcript extending from exon 1 to the inserted vector, but also transcripts that spliced directly from exon 1 to exon 3, bypassing the fusion between the gene-trap vector and exon 2 (Fig. 2B). This indicates that transcription termination within the gene-trap vector is not absolute. However, because these transcripts lack exon 2 (confirmed by sequencing the PCR products), any translation product would be expected to be non-functional because of the absence of the 25 amino acids encoded by this exon. Structural studies indicate that these 25 residues – a significant fraction of the total 101 amino acids in mature SUMO1 – contribute to the first β-sheet making up the ubiquitin fold (Bayer et al., 1998; Jin et al., 2001) and interact with the SUMO E2 conjugating enzyme, Ubc9 (Capili and Lima, 2007; Duda and Schulman, 2005).

To confirm disruption at the protein level, we carried out immunoblotting of whole cell extracts prepared from embryos dissected at several different developmental stages using polyclonal anti-SUMO1 antisera. Our analysis showed a complete lack of high molecular mass SUMO1 conjugates in XA024 homozygotes and a significantly reduced level in heterozygotes (Fig. 3A, upper panel). We also were unable to detect free SUMO1 in homozygotes (Fig. 3A, lower panel). To confirm that our inability to detect SUMO1 was indeed due to lack of expression and not lack of recognition by our antisera of the truncated protein, we generated a SUMO1 expression construct carrying the same internal deletion of amino acids encoded by exon 2. This construct was His-tagged for bacterial expression and purification, with the purified protein then analyzed by immunoblotting. As shown in supplementary material Fig. S2A, anti-SUMO1 antiserum recognizes the internally truncated protein as efficiently as it does the full-length SUMO1. The same construct was also pyo-tagged and used for transient transfection of HEK293 cells. However, we were unable to detect expression by immunoblotting (supplementary material Fig. S2B), suggesting

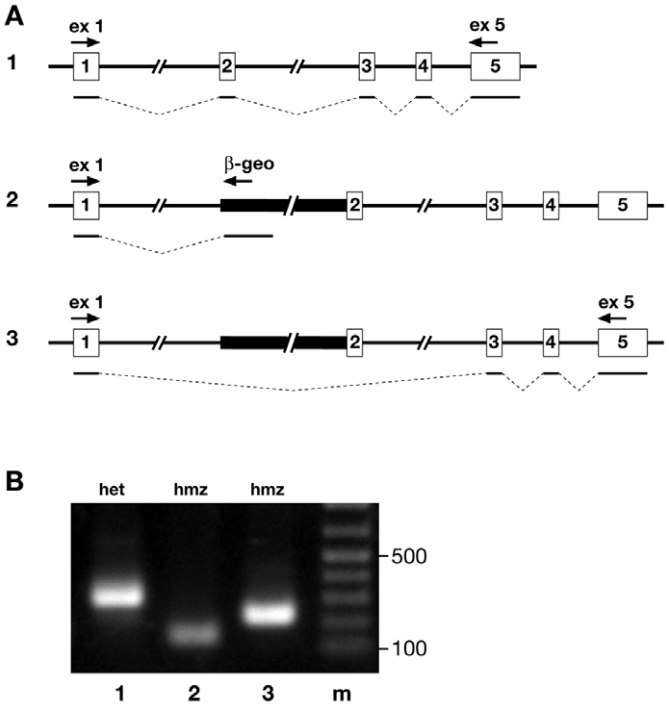

Fig. 2. RT-PCR analysis of splicing products. (A) Schematic representation of the *SUMO1* gene with various primer sets (arrows) used to detect (1) the normal spliced transcript; (2) the transcript splicing into the gene trap vector; (3) the transcript skipping the vector and truncated exon 2. (B) Agarose gel showing RT-PCR products generated using the primer sets shown in A and RNA derived from E15.5 embryos of the indicated genotype. het, heterozygous; hmz, homozygous. The lane numbers correspond to the primer sets in A. m, 100 bp ladder molecular size marker.

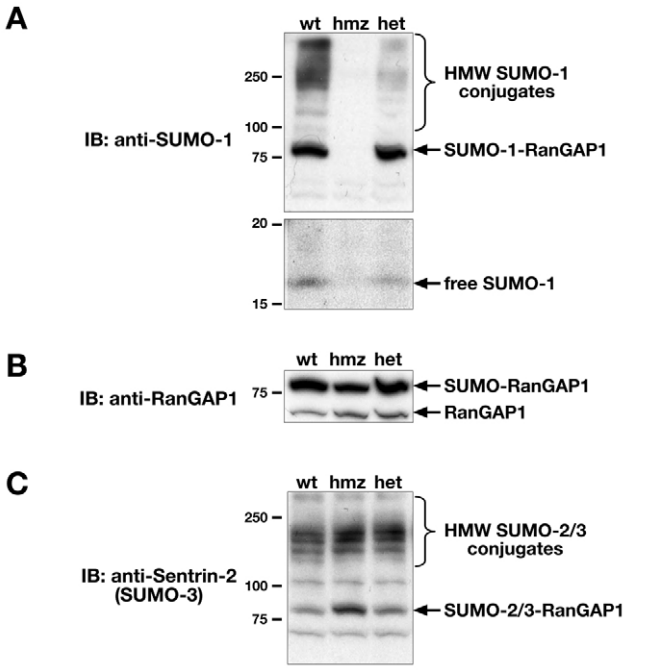

Fig. 3. Immunoblot analysis of sumoylation. The genotypes are shown above the lanes; wt, wild type; hmz, homozygous; het, heterozygous. Molecular mass in kilodaltons (kDa) is shown to the left of each panel. (A) Whole-embryo extracts immunoblotted with anti-SUMO1 antibody. There is complete lack of high molecular mass SUMO1 conjugates (upper panel) and free SUMO1 (lower panel) in homozygotes, and reduced levels in heterozygotes. (B) Same blot as in upper panel of A, reanalyzed with anti-RanGAP1 antibody. Sumoylated form of RanGAP1 is present even in homozygotes. (C) Whole-embryo extracts immunoblotted with anti-SUMO3 antibody. Band at the position of sumoylated RanGAP1 (>75 kDa) is more intense in homozygotes. Higher molecular mass SUMO2/3 conjugates are essentially unchanged.

that the internally deleted SUMO1 is poorly expressed and/or unstable. Together, these results indicate that XA024 represents a true loss-of-function SUMO1 gene-trap allele.

No loss of SUMO1 function in RRQ016 gene-trap mice

The lack of any effect on normal development and homeostasis in the absence of SUMO1 is contrary to a previous report (Alkuraya et al., 2006). In an attempt to resolve these differences, we also derived mice from RRQ016 ES cells. We were able to map the vector insertion site in this line, also within the *SUMO1* first intron, using the same strategy as for XA024. However, our analysis revealed a complex rearrangement involving an apparent duplication of at least 3 kb of host sequence from the preintegration site (supplementary material Fig. S3), which presumably occurred at the time of gene-trap vector insertion. This prevented straightforward PCR genotyping of heterozygotes compared with homozygotes, as used for XA024-derived mice. Therefore, we used alternative approaches to predict genotypes. From matings of obligate heterozygotes, we determined the ratio of β-geo-positive embryos and pups to wild-type controls. An analysis of close to 100 offspring showed a 3:1 ratio, consistent with the β-geo-positive pool containing both gene-trap heterozygotes and homozygotes. Indeed, X-gal staining of embryos allowed us to distinguish two classes based on staining intensity, with the more strongly stained embryos being presumptive homozygotes (supplementary material Fig. S4). Importantly, none of the embryos or pups showed any phenotypic defects. As a second approach, we outbred β-geo-positive animals to wild-type mice and identified individuals whose offspring all were β-geo-positive, genetic evidence that the individuals being outbred were homozygous for the RRQ016 gene-trap insertion. Together, these data indicate that homozygotes develop to term and are normal and fertile.

Somewhat surprisingly, immunoblotting of protein extracts from a large number of embryos derived from these crosses revealed no changes in SUMO1 conjugation in any β-geo-positive embryo (heterozygote or presumptive homozygote), indicating that despite the complex rearrangement in the first intron, *SUMO1* expression is not affected in RRQ016 derived mice (supplementary material Fig. S5). Thus, we cannot duplicate the results of the previous study. The defects observed by Alkuraya et al. (Alkuraya et al., 2006), therefore, must be due to mutation of another gene, with this mutation either having arisen independently or having been lost in our RRQ016-derived mice.

Compensatory sumoylation of RanGAP1 by SUMO2/3

Our data indicate that mutation of SUMO1 is found only in XA024-derived and not in RRQ016-derived animals. Therefore, to understand the molecular consequences of loss of SUMO1 function, we carried out further analyses only on the XA024 line. We first addressed sumoylation of RanGAP1, to which the majority of SUMO1 in normal cells is conjugated. In addition,

the majority of RanGAP1 normally is sumoylated, unlike other SUMO targets for which only a minor fraction is conjugated at any one time. Thus, sumoylated RanGAP1 is easily detected as a ~90 kDa species in anti-SUMO1 immunoblots of whole-embryo extracts (Fig. 3A upper panel, arrow). As expected, we found no band at that position for XA024 homozygotes. However, when the same blots were reanalyzed with anti-RanGAP1 antisera, we were surprised to find that all samples, even homozygotes, showed the higher molecular mass, presumably sumoylated, form (Fig. 3B). To determine whether RanGAP1 is sumoylated with SUMO2 or SUMO3, we examined the same samples with polyclonal anti-sentrin-2 (SUMO3), which recognizes both of these nearly identical SUMO isoforms. Indeed, we found a sumoylated species with a molecular mass appropriate for sumoylated RanGAP1 in all samples, the levels of which were higher in XA024 homozygotes (Fig. 3C). This suggested that SUMO2 and/or SUMO3 is normally conjugated to RanGAP1, with the level increasing in the absence of SUMO1. Interestingly, there did not appear to be any significant increase in higher molecular mass SUMO2/3 conjugates in XA024 homozygotes, suggesting that relatively few additional proteins become conjugated with SUMO2/3 in the absence of SUMO1.

To confirm sumoylation of RanGAP1 by SUMO2/3, we immunoprecipitated total RanGAP1 and determined the presence of different SUMO conjugates by immunoblotting with isoform-specific antisera (Fig. 4). As expected, analysis with anti-SUMO1 antibody detected RanGAP1 SUMO1 conjugates only in wild-type and XA024 heterozygous embryos, not in homozygotes (Fig. 4B, right panel). Analysis with a different polyclonal antibody against SUMO2/3 (anti-SUMO2) confirmed that, in addition to the large pool conjugated with SUMO1, there is normally some RanGAP1 sumoylated with SUMO2 and/or SUMO3 (Fig. 4C, right panel). The intensity of the band corresponding to the RanGAP1 SUMO2/3 conjugate was clearly stronger in the XA024 homozygote indicating an increase in response to loss of SUMO1 conjugation. Analysis of the corresponding whole embryo extracts with polyclonal anti-SUMO2 gave somewhat different results to those seen above with polyclonal anti-Sentrin-2 (SUMO3), which is not surprising, because we have noticed differences in the specificity of these two antisera previously (Yamaguchi et al., 2005). With anti-SUMO2 antibody, we saw a clear shift to a higher average molecular mass for SUMO2/3 conjugates in the absence of SUMO1 (Fig. 4C, left panel). This could reflect increased SUMO2/3 chain length (Tatham et al., 2001) as a result of the absence of potentially chain-terminating SUMO1 (Fu et al., 2005) on normal SUMO2/3 targets.

Decreased localization of SUMO2/3 modified RanGAP1 to the nuclear pore

Examination of the same samples with anti-RanGAP1 antibody showed a lower overall level of sumoylated RanGAP1 in XA024 homozygotes (Fig. 4A). This decrease could be due either to sumoylation with SUMO2/3 being less efficient than with SUMO1 or to a higher rate of desumoylation. Sumoylation of RanGAP1 is essential for its interaction with RanBP2 and localization to nuclear pore complexes (NPCs) (Mahajan et al., 1997; Matunis et al., 1996). To test whether decreased RanGAP1 sumoylation leads to reduced NPC localization in XA024 homozygotes, we derived primary mouse embryo fibroblasts (MEFs) from wild-type, heterozygous and homozygous littermates and carried out immunofluorescence studies. We found that RanGAP1 localized at the nuclear rim in all samples regardless of genotype (Fig. 5A-C). However, the amount seen in XA024 homozygous MEFs was clearly less than that in wild-type and heterozygous MEFs, consistent with the overall reduced levels of sumoylated RanGAP1. Immunofluorescence also confirmed the absence of SUMO1 in XA024 homozygous MEFs (Fig. 5D-F), while showing no significant change in level or subcellular localization of SUMO2/3 (Fig. 5G-I). This again suggests only limited numbers of additional proteins undergoing conjugation with SUMO2/3 in the absence of SUMO1.

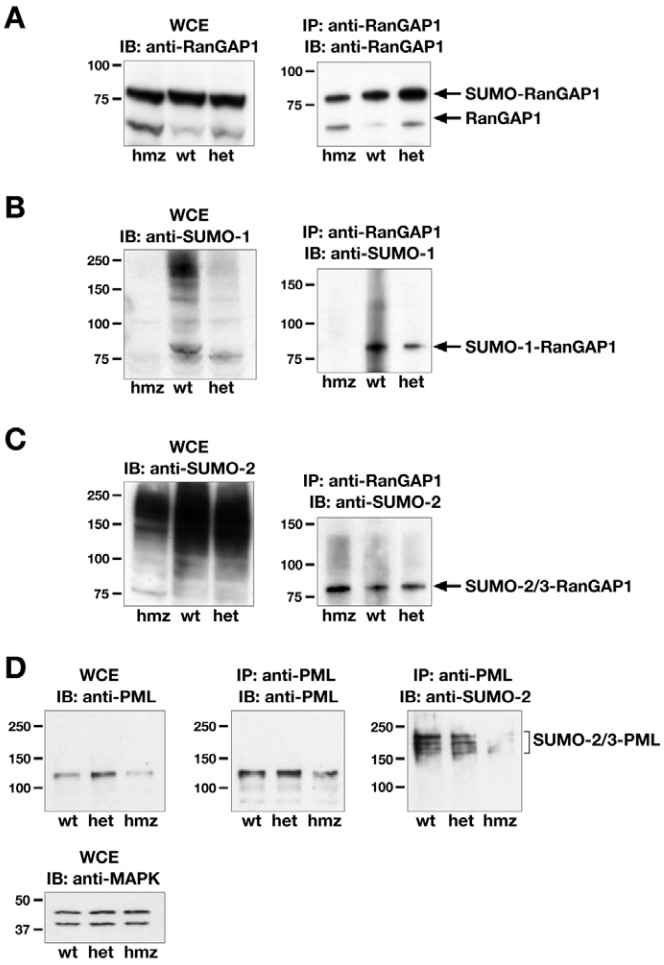

Fig. 4. Immunoblot analysis of RanGAP1 and PML sumoylation. (A,B) Whole-cell extracts (WCE) from embryos are shown in left panels, and immunoprecipitation (IP) with anti-RanGAP1 antibody shown in right panels. The genotypes are shown below lanes; hmz, homozygous; wt, wild type; het, heterozygous. There is less sumoylated form in the homozygote both in WCE and IP upon analysis with anti-RanGAP1 antibody (A). IP shows less sumoylated form in the heterozygote and none in homozygote analysis with anti-SUMO1 antibody (B). (C) Analysis with anti-SUMO2 antibody. The immunoprecipitation shows more sumoylated form in the homozygotes compared to the wild type and heterozygotes. The whole cell extract shows an increase in average molecular mass of SUMO2/3 high molecular mass conjugates in homozygotes. (D) Whole cell extracts (WCE) from MEFs immunoblotted with anti-PML antibody (left). Reblotting with anti-MAPK (lower panel) shows equivalent loading of heterozygous and homozygous samples but less protein loaded for the wild-type sample. Therefore, there is less total PML in the homozygote. Immunoprecipitation (IP) of extracts with anti-PML antibody is shown in the middle and right panels. Immunoblotting with anti-PML antibody is shown in the middle panel and with anti-SUMO2 in the right panel. There is less SUMO2/3 conjugation of PML in MEFs derived from XA024 homozygotes.

Loss of SUMO1 affects PML levels and PML nuclear body formation

Another major target of SUMO1 is the promyelocytic leukemia (PML) protein (Muller et al., 1998; Sternsdorf et al., 1997), with sumoylation of PML required for its assembly into subnuclear structures known as PML nuclear bodies and the recruitment of other nuclear-body-associated proteins (Bernardi and Pandolfi, 2007). PML also is sumoylated by SUMO2/3, with recent evidence indicating that the formation of poly-SUMO2/3 chains is critical for PML nuclear body formation and/or maintenance (Fu et al., 2005; Mukhopadhyay et al., 2006). To examine the effects of loss of SUMO1 on PML we carried out immunoblotting on samples from embryos and MEFs (Fig. 4D). Surprisingly, we consistently found a reduced amount of PML in XA024 homozygotes (Fig. 4D, upper left panel and middle panel). To examine sumoylation of PML by SUMO2/3, we immunoprecipitated total PML and immunoblotted with anti-SUMO2. Unlike results found for RanGAP1, there was significantly less sumoylation of PML with SUMO2/3 in homozygotes compared with wild type (Fig. 4D, right panel). Interestingly, the decrease in sumoylation levels appears even greater than the decrease in overall PML levels, suggesting reduced steady state SUMO2/3 conjugation. Recent work has shown that PML turnover is regulated by the ubiquitin ligase RNF4, which recognizes poly-SUMO2/3 chains on PML (Lallemand-Breitenbach et al., 2008; Tatham et al., 2008). If SUMO1 indeed normally acts as a chain terminator (Fu et al., 2005), its absence might more readily allow formation of poly-SUMO2/3 chains long enough to be efficiently recognized by RNF4, leading to higher turnover rates.

Because of the importance of PML sumoylation for PML nuclear body formation and stability, we carried out immunofluorescence on MEFs using anti-PML antisera (Fig. 5J-L). Given the lower overall levels of PML in SUMO1 mutants, it was not surprising to find fewer PML nuclear bodies in MEFs derived from XA024 homozygotes. Whereas there were approximately 19 PML nuclear bodies per cell in wild-type MEFs and 15 PML nuclear bodies per cell in XA024 heterozygous MEFs, only ~10 per cell were found in XA024 homozygous MEFs (supplementary material Table S1). These data indicate that formation of PML nuclear bodies can occur in the absence of SUMO1, but overall numbers are significantly reduced.

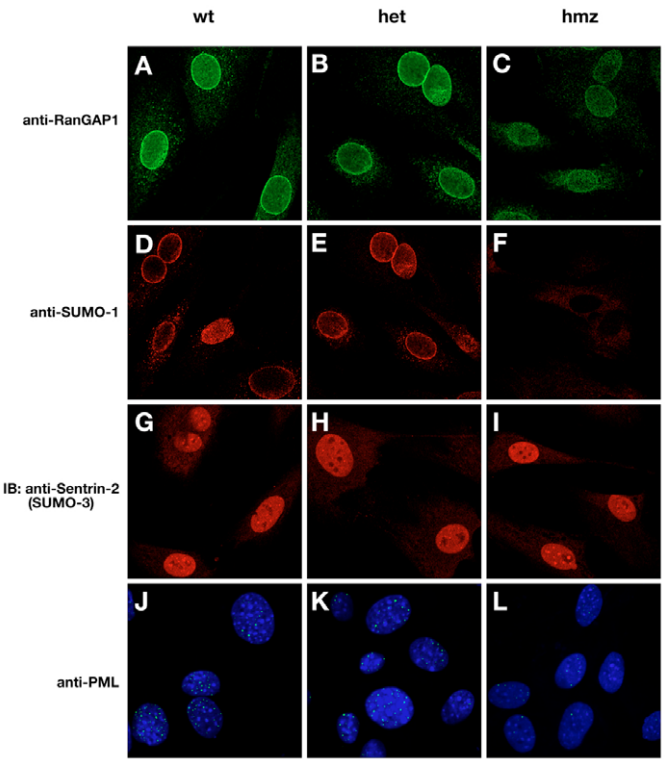

Fig. 5. Immunofluorescence analysis of XA024 MEFs. The genotypes are shown above panels; wt, wild type; het, heterozygous; hmz, homozygous. (A-C) Analysis with anti-RanGAP1 antibody. There is decreased nuclear rim staining in the homozygote (C) compared with the wild type (A) or heterozygote (B). (D-F) Analysis with anti-SUMO1 antibody. Staining in wild type (D) and heterozygote (E) is predominantly nuclear and nuclear rim. There is no staining above background in homozygote (F). (G-H) Analysis with anti-Sentrin 2 (SUMO3) antibody. There is no change in staining intensity or pattern in hetero- (H) and homozygotes (I) compared with the wild type (G). (J-L) Analysis with anti-PML antibody. Fewer PML nuclear bodies are observed in homozygote (L) compared with the wild type (J) and heterozygote (K).

Discussion

Our results convincingly show that loss of SUMO1 has no significant effect on either embryonic development or homeostasis. This is probably due to compensatory sumoylation of SUMO1 targets by SUMO2 and/or SUMO3. We have shown this to be the case for the major SUMO1 target RanGAP1. Our studies show that normally there is a low level of RanGAP1 sumoylation with SUMO2 and/or SUMO3, and this becomes significantly increased in the absence of SUMO1. The fact that compensation by SUMO2/3 occurs suggests that a critical threshold level of RanGAP1 sumoylation is normally required. Although whole-animal studies examining the consequences of unsumoylated RanGAP1 have not been reported, an overall lack of sumoylation resulting from targeted mutation of *Ubc9* in the mouse results in alterations in the subcellular distribution of RanGAP1, disrupting the establishment and maintenance of the RanGTPase gradient essential for nucleocytoplasmic transport. This, along with a number of other severe defects seen in *Ubc9*-mutant cells, no doubt leads to the early preimplantation arrest of mutant embryos (Kuehn, 2005; Nacerddine et al., 2005). Thus, redundancy of function of SUMO isoforms might be an important cellular strategy to maintain threshold levels of sumoylation for key proteins. The number of such proteins is hard to predict. The limited changes we see in the SUMO2/3 sumoylation pattern in SUMO1 mutants, might argue against extensive compensation. However, for most proteins that are sumoylated, only a small fraction of the total pool is in the conjugated state at any one time. Thus, even a large number of additional targets might represent only a minimal contribution to the normal set of SUMO2/3 conjugates. Ultimately, a proteomic analysis will be necessary to resolve this question. It will also be of interest to determine whether SUMO1 can compensate for loss of SUMO2/3 function, both in terms of mono- and poly-sumoylation. This will require development of SUMO2 and SUMO3 mutant strains and the production of compound heterozygotes and homozygotes.

Our results show that RanGAP1 sumoylation with SUMO2/3 is less efficient and/or less stable than with SUMO1, and that there is reduced nuclear pore localization of RanGAP1 exclusively conjugated with SUMO2/3. In addition, the lack of SUMO1 leads to reduced PML levels and significantly fewer PML nuclear bodies. There might also be changes in the activity, stability or localization of other SUMO1 targets. Although under normal physiological

conditions we find no apparent detrimental effects, it is possible that under conditions of stress the lack of SUMO1 could have a significant impact on normal embryonic development or homeostasis. It is known that SUMO2/3 conjugation increases under conditions of heat shock and other protein-damaging conditions (Saitoh and Hinchey, 2000). Such conditions might reduce the levels of SUMO2/3 available for compensatory conjugation to normal SUMO1 targets, thereby reducing the amount of the sumoylated form below critical thresholds. Thus, an important avenue for further study will be to examine SUMO1-deficient cells and mice under various stress conditions.

We recently showed that mutation of the SUMO protease SENP1 results in a significant increase in steady state levels of a range of SUMO1-conjugated proteins, leading to placental abnormalities associated with overproliferation of trophoblast (Yamaguchi et al., 2005). We found no changes in the level of SUMO2/3-conjugated proteins, indicating that SENP1 uniquely desumoylates SUMO1-conjugated proteins and its activity cannot be compensated for by any of the other five SUMO proteases. Studies on other desumoylating enzymes have also revealed a similar degree of specificity (Mukhopadhyay and Dasso, 2007). Along with the results presented here showing that SUMO2/3 can effectively replace SUMO1, this suggests that specificity in the sumoylation pathway resides predominantly in the action of E3s and desumoylating enzymes, rather than in the isoforms themselves. This has important implications for any effort to develop rational approaches for targeting the SUMO pathway. Based on recent findings showing an association between sumoylation and carcinogenesis and metastasis (Baek, 2006; Cheng et al., 2006; Katayama et al., 2007; Kim and Baek, 2006; Moschos and Mo, 2006; Seeler et al., 2007; Wu and Mo, 2007), targeting the SUMO pathway for cancer therapy has been proposed (Mo and Moschos, 2005). The fact that SUMO family members can substitute for each other suggests that components of the pathway other than SUMO, perhaps the deconjugation enzymes, might be the most effective targets for rational drug development.

Materials and Methods

Cells and mice

BayGenomics ES cells XA024 and RRQ016 were obtained from the Mutant Mouse Regional Resource Center at University of California, Davis, and maintained as described on the International Gene Trap Organization (IGTO) website (http://www.genetrap.org). Chimeric mice were made by blastocyst injection following standard protocols. Mouse embryo fibroblasts (MEFs) were isolated from embryonic day (E)12.5 embryos by established procedures and maintained in 3% O_2 as described (Parrinello et al., 2003).

Gene-trap structure determination and genotyping analysis

The sites of gene-trap vector insertions in XA024 and RRQ016 lines were confirmed using a 5′ rapid amplification of cDNA ends (RACE) kit (Roche, Basel, Switzerland), according to the protocols provided by the manufacturer and using the general strategy and primers outlined on the IGTO website. To identify the point of gene-trap vector insertion, we carried out long-range PCR using a series of forward primers starting in exon 1 (5′-TGAATCCACGTCACCATGTC-3′) and continuing every 3000 bp along the length of the first intron (5′-ATTTCTGCTGGTCTTGGTAAC-3′, intron position 3039; 5′-AAAGGCTGCACTACCTCACG-3′, intron position 6008; 5′-TTGGCAGAAGATTAACCAGC-3′, intron position 8998; 5′-CAGGAAGAAGCAACTCTTGAC-3′, intron position 11966; 5′-AGAGTGAGTTCCAGGACAGC-3′, intron position 14732), along with a reverse primer specific for the gene-trap vector (5′-CGACGGGATCCTCTAGAGTC-3′) (Fig. 1). To determine the 3′ junction, we used forward primers specific for the 3′ end of the gene-trap vector (5′-GTTCGGTGTAGGTCGTTCGCTCCAAG-3′, position 9398; 5′-GTGAGGCACCTATCTCAGCGATCTGTCTATTTC-3′, position 9956; 5′-GCGACCGAGTTGCTCTTGCCCG-3′, position 10527) and a reverse primer specific for exon 2 (5′-CGCCTAAGTCCTCAGTTGAAGGTTTTGC-3′). To genotype XA024 mice, we utilized a forward primer located in the gene-trap vector (5′-GGCTGGCTTAACTATGCGGCATCAGAG-3′, position 11134) along with the exon 2 reverse primer to amplify the gene-trap allele. A forward primer located in intron 1 close to the insertion site (5′-TCCACCTGCCTCTACCTCAAGTGCTG-3′, position 15061), was used with the exon 2 reverse primer to amplify the wild-type allele.

A similar long-range PCR strategy was used to determine the site of insertion of the gene-trap vector in the RRQ016 line. For genotyping, a forward primer specific to intron 1 (5′-TTTAGGCAGGCAGTGATGGCATACACC-3′, position 10599) was used with a reverse primer specific for the gene-trap vector (5′-CGCATCGTAACCGTGCATCTGCCAG-3′, position 1904) to amplify the gene-trap allele. The intron-1-specific primer was used with a reverse primer from intron 1 (5′-GCCATCTCACCAGCCCGTCTTGGATC-3′, position 11282) to amplify the wild-type allele.

For SUMO1 transcript analysis by RT-PCR (Fig. 2), first strand cDNA was synthesized from total RNA isolated from E12.5 wild type and mutant fetuses using oligo(dT)20 primer and SuperScript III First-Strand Synthesis System (Invitrogen, Carlsbad, CA) according to protocols provided by manufacturer. Primers specific for exon 1 (5′-GTGAATCCACGTCACCATGTC-3′) and exon 5 (5′-CCGTTTGTTCCTGATAAACTTC-3′) were used to amplify the normal *SUMO1* mRNA transcript. The same exon 1 primer was used with a β-geo specific primer (5′-CGACGGGATCCTCTAGAGTC-3′) to amplify the fusion transcript.

Immunoblotting, immunoprecipitation and antibodies

To prepare whole embryo protein extracts, dissected embryos were washed in 1× PBS and snap-frozen in liquid nitrogen. To each sample, 800 μl of lysis buffer (50 mM Tris-HCl pH 8.0, 150 mM NaCl, 2 mM EDTA, 3% SDS, 1% sodium deoxycholate) was added, followed by sonication and centrifugation. Protein concentrations were determined using BCA protein assay kit (Pierce, Rockford, IL). For each sample, 40 μg was fractionated on a 4-12% NuPAGE gel followed by transfer to PVDF membrane and analysis with appropriate antibodies. For immunoprecipitation, 0.5 mg of total protein diluted to a final concentration of 0.5 mg/ml with dilution buffer (100 mM Tris pH 7.5, 150 mM NaCl, 2 mM EDTA, 1% Triton X-100, protease inhibitors) was pre-cleared with Protein-G-Sepharose beads (Amersham Biosciences, Uppsala, Sweden) for 30 minutes at 4°C. The beads were removed and appropriate primary antibody was added, incubated for 2 hours at 4°C on a rotary platform followed by incubation for 1 hour with new Protein-G-Sepharose beads. The beads were pelleted by centrifugation, washed three times with dilution buffer, resuspended in 4× NuPAGE sample buffer and loaded on 4-12% NuPAGE gels for immunoblot analysis with appropriate antibodies.

To prepare total cell extracts from MEFs, cells were collected in 62.5 mM Tris-HCl pH 6.8. An equal amount of 2× SDS sample buffer (62.5 mM Tris-HCl pH 6.8, 10% glycerol, 6% SDS, 1 mM PMSF, 10 mM iodoacetamide and protease inhibitors) was added followed by sonication and centrifugation. For immunoprecipitation, approximately 1 mg of protein was diluted 10 times with Triton X-100 lysis buffer (50 mM Tris-HCl pH 7.5, 150 mM NaCl, 1 mM EDTA, 0.5% Triton X-100, 1 mM PMSF, 10 mM iodoacetamide and protease inhibitors), precleared with protein-G-agarose beads for 1 hour at 4°C, followed by addition of appropriate primary antibody. After incubation at 4°C overnight, immunoprecipitates were washed three times with 1 ml of the above Triton X-100 lysis buffer, and subsequently resuspended in 2× SDS sample buffer. After boiling for 10 minutes, the samples were evaluated by immunoblotting.

To generate anti-SUMO1 antibody, we cloned a GST-SUMO1 fusion construct into the pGEX-4T-2 vector and expressed protein in *E. coli*. GST-SUMO1 protein was purified over Glutathione-Sepharose beads and injected into rabbits by standard methods. The antibody was affinity purified by passing sera over a HiTrap NHS-activated HP FPLC affinity column (GE Healthcare, Pittsburg, PA), conjugated with purified SUMO1 prepared by thrombin digestion of the fusion protein. Bound antibody was released from the column with 0.2 M glycine solution (pH 2.4) and immediately neutralized with 2 M Tris base (pH 9.0). Fractions containing the highest amount of antibody were pooled and dialyzed overnight against PBS, then concentrated using Centricon YM-10 columns (Millipore, Billerica, MA). Other primary antibodies included a second rabbit polyclonal anti-SUMO1 and rabbit polyclonal anti-SUMO2 (gift from Mary Dasso), rabbit polyclonal anti-Sentrin-2 (SUMO3) (Invitrogen, Carlsbad, CA), mouse monoclonal RanGAP1 (Invitrogen), and mouse monoclonal anti-PML (clone 36.1-104; Millipore). Mouse monoclonal anti-β-actin (Sigma, St. Louis, MO) or rabbit polyclonal anti-p44/42 MAP kinase (Cell Signaling Technology, Beverly, MA) was used to confirm equivalent protein loading. Detection of the secondary antibody-HRP conjugates was done using ECL plus Western Blotting Detection system (Amersham Biosciences). Blots were stripped using Restore Western Blot Stripping buffer (Pierce) according to the manufacturer's specifications.

X-gal staining

Embryos were isolated, washed in 1× PBS and fixed in 1% formaldehyde, 0.2% glutaraldehyde, 0.02% NP-40 in PBS for 2 hours on ice, followed by three 15 minute incubations in 1× PBS solution, containing 2 mM $MgCl_2$ and 0.02% NP-40 at room temperature. Staining was carried out overnight in 320 μg/ml X-gal, 12 mM $K_3Fe(CN)_6$, 12 mM $K_4Fe(CN)_6$, 0.002% NP-40, 4 mM $MgCl_2$ in PBS at 37°C on a rocking platform. After staining, embryos were washed twice for 30 minutes each, in 0.2% NP-40 in PBS. To improve visualization of β-galactosidase expression, embryos were cleared in a series of solutions containing 20%, 50% and 80% glycerol

(v/v) diluted with 1% KOH (w/v) (Schatz et al., 2005). Each incubation step was carried out for 2 weeks at 30°C with gentle rocking, followed by transfer to 80% glycerol in PBS for imaging. Selected embryos were imaged using a Zeiss AxioCam MRc5 camera and AxioVision software through a Leica MZ16 stereomicroscope.

Immunofluorescence studies

MEFs were seeded in glass slide incubation chambers at 1×10^5 per well. The following day, cells were fixed for 10 minutes with 4% formaldehyde in PBS and washed three times with PBS. Cells then were permeabilized for 5 minutes on ice in PBS containing 0.2% Triton X-100 and 1% normal goat serum (NGS) followed by three 10 minute washes with 1% NGS in PBS. Samples were incubated with appropriate primary antibody overnight at 4°C. The next day, cells were washed three times in PBS for 10 minutes each, then incubated with secondary antibody for 1 hour at room temperature, followed by another set of washes in PBS. Cells were incubated with Hoechst 33258 dye (1:5000 dilution; Invitrogen) for 10 minutes at room temperature and washed twice with PBS for 5 minutes each. Samples were visualized using a Zeiss LSM510 confocal microscope (Carl Zeiss, Jena, Germany) with all images acquired using identical parameters. Cell nuclei were semi-automatically segmented using a dynamic programming method (Baggett et al., 2005). PML nuclear bodies were automatically detected using a modification of a method based on multi-scale products (Olivo-Marin, 2002).

cDNA constructs and expression analysis

To confirm the specificity of the anti-SUMO1 antibody we generated *SUMO1* cDNA expression constructs that were full length or internally deleted as in XA024 (lacking amino acids EAKPSTEDLGDKKEGEIKLKVIGQ encoded by exon 2). The truncated *SUMO1* construct was created using primers specific for the first and the last exons of *SUMO1* and first strand cDNA from a homozygous mutant fetus as a template. After digestion with appropriate restriction enzymes, truncated *SUMO1* construct was ligated into pcDNA3.1(–) along with a pyo epitope tag for mammalian expression, and into pRSFDuet along with a 6×His tag for bacterial expression and purification.

E. coli BL21 (DE3) cells transformed with pRSFDuet expressing either full-length or truncated His-tagged SUMO1 were grown overnight at 37°C in LB broth. Overnight cultures were diluted 50-fold into LB supplemented with 25 μg/ml of kanamycin and grown at 37°C to 0.8 OD at 600 nm, then induced with IPTG at a final concentration of 1 mM. After 3 hours, cells were harvested and lysed by sonication in Buffer A (0.1 M phosphate buffer pH 7.8, 0.3 M NaCl, 8 M urea). Cell debris was removed by centrifugation at 20,000 ***g*** for 20 minutes and the supernatant was incubated with Talon beads (Invitrogen) for 1 hour at room temperature. After incubation, beads were washed three times with Buffer A and purified protein was eluted off the beads with Buffer A supplemented with 0.3 M imidazole. Purified proteins were analyzed by immunoblotting with anti-SUMO1 antibody. For mammalian expression, HEK293 cells were transiently transfected with plasmids encoding either full-length or truncated pyo-SUMO1 using Lipofectamine 2000 (Invitrogen). After 24 hours, cells were collected and sonicated in lysis buffer (50 mM Tris pH 7.5, 0.15 M NaCl, 2 mM EDTA, 0.05% sodium deoxycholate, 3% SDS), followed by centrifugation. Samples were analyzed by immunoblotting with anti-SUMO1 and anti-pyo antisera.

We thank the NCI CCR Gene Targeting Facility for generation of chimeric mice; Mary Dasso (NICHD, Bethesda, MD) for antibodies and advice; Prabhakar Gudla and Kaustav Nandy of the NCI-Frederick Optical Microscopy and Analysis Laboratory who developed the automatic method to detect the PML bodies and made the Baggett nuclear segmentation method into a practical, user-friendly tool, respectively; George Lezin for help with PCR methodology; Allan Weissman and members of his laboratory for discussion; and Shyam Sharan, Alessandra Mazzoni, Amit Kumar and Øyvind Dahle for comments on the manuscript. This work was supported by the Intramural Research Program of the National Institutes of Health, National Cancer Institute, Center for Cancer Research and with federal funds from the National Cancer Institute, National Institutes of Health under Contract N01-CO-12400. The content of this publication does not necessarily reflect the views or policies of the Department of Health and Human Services and nor does mention of trade names, commercial products or organizations imply endorsement by the US Government. NCI-Frederick is accredited by AAALAC International and follows the Public Health Service Policy for the Care and Use of Laboratory Animals. Animal care was provided in accordance with the procedures outlined in the 'Guide for Care and Use of Laboratory Animals' (National Research Council 1996).

References

Alkuraya, F. S., Saadi, I., Lund, J. J., Turbe-Doan, A., Morton, C. C. and Maas, R. L. (2006). SUMO1 haploinsufficiency leads to cleft lip and palate. *Science* **313**, 1751.

Ayaydin, F. and Dasso, M. (2004). Distinct *in vivo* dynamics of vertebrate SUMO paralogues. *Mol. Biol. Cell* **15**, 5208-5218.

Baek, S. H. (2006). A novel link between SUMO modification and cancer metastasis. *Cell Cycle* **5**, 1492-1495.

Baggett, D., Nakaya, M. A., McAuliffe, M., Yamaguchi, T. P. and Lockett, S. (2005). Whole cell segmentation in solid tissue sections. *Cytometry A* **67**, 137-143.

Bayer, P., Arndt, A., Metzger, S., Mahajan, R., Melchior, F., Jaenicke, R. and Becker, J. (1998). Structure determination of the small ubiquitin-related modifier SUMO-1. *J. Mol. Biol.* **280**, 275-286.

Bernardi, R. and Pandolfi, P. P. (2007). Structure, dynamics and functions of promyelocytic leukaemia nuclear bodies. *Nat. Rev. Mol. Cell. Biol.* **8**, 1006-1016.

Capili, A. D. and Lima, C. D. (2007). Structure and analysis of a complex between SUMO and Ubc9 illustrates features of a conserved E2-Ubl interaction. *J. Mol. Biol.* **369**, 608-618.

Cheng, J., Bawa, T., Lee, P., Gong, L. and Yeh, E. T. (2006). Role of desumoylation in the development of prostate cancer. *Neoplasia* **8**, 667-676.

Duda, D. M. and Schulman, B. A. (2005). Tag-team SUMO wrestling. *Mol. Cell* **18**, 612-614.

Fu, C., Ahmed, K., Ding, H., Ding, X., Lan, J., Yang, Z., Miao, Y., Zhu, Y., Shi, Y., Zhu, J. et al. (2005). Stabilization of PML nuclear localization by conjugation and oligomerization of SUMO-3. *Oncogene* **24**, 5401-5413.

Geiss-Friedlander, R. and Melchior, F. (2007). Concepts in sumoylation: a decade on. *Nat. Rev. Mol. Cell. Biol.* **8**, 947-956.

Gill, G. (2004). SUMO and ubiquitin in the nucleus: different functions, similar mechanisms? *Genes Dev.* **18**, 2046-2059.

Girdwood, D. W., Tatham, M. H. and Hay, R. T. (2004). SUMO and transcriptional regulation. *Semin. Cell Dev. Biol.* **15**, 201-210.

Hay, R. T. (2005). SUMO: a history of modification. *Mol. Cell* **18**, 1-12.

Jin, C., Shiyanova, T., Shen, Z. and Liao, X. (2001). Heteronuclear nuclear magnetic resonance assignments, structure and dynamics of SUMO-1, a human ubiquitin-like protein. *Int. J. Biol. Macromol.* **28**, 227-234.

Johnson, E. S. (2004). Protein modification by SUMO. *Annu. Rev. Biochem.* **73**, 355-382.

Katayama, A., Ogino, T., Bandoh, N., Takahara, M., Kishibe, K., Nonaka, S. and Harabuchi, Y. (2007). Overexpression of small ubiquitin-related modifier-1 and sumoylated Mdm2 in oral squamous cell carcinoma: possible involvement in tumor proliferation and prognosis. *Int. J. Oncol.* **31**, 517-524.

Kerscher, O., Felberbaum, R. and Hochstrasser, M. (2006). Modification of proteins by ubiquitin and ubiquitin-like proteins. *Annu. Rev. Cell Dev. Biol.* **22**, 159-180.

Kim, K. I. and Baek, S. H. (2006). SUMOylation code in cancer development and metastasis. *Mol. Cells* **22**, 247-253.

Kuehn, M. R. (2005). Mouse Ubc9 knockout: many path(way)s to ruin. *Dev. Cell* **9**, 727-728.

Lallemand-Breitenbach, V., Jeanne, M., Benhenda, S., Nasr, R., Lei, M., Peres, L., Zhou, J., Zhu, J., Raught, B. and de The, H. (2008). Arsenic degrades PML or PML-RARalpha through a SUMO-triggered RNF4/ubiquitin-mediated pathway. *Nat. Cell Biol.* **10**, 547-555.

Lin, D. Y., Huang, Y. S., Jeng, J. C., Kuo, H. Y., Chang, C. C., Chao, T. T., Ho, C. C., Chen, Y. C., Lin, T. P., Fang, H. I. et al. (2006). Role of SUMO-interacting motif in Daxx SUMO modification, subnuclear localization, and repression of sumoylated transcription factors. *Mol. Cell* **24**, 341-354.

Mahajan, R., Delphin, C., Guan, T., Gerace, L. and Melchior, F. (1997). A small ubiquitin-related polypeptide involved in targeting RanGAP1 to nuclear pore complex protein RanBP2. *Cell* **88**, 97-107.

Matunis, M. J., Coutavas, E. and Blobel, G. (1996). A novel ubiquitin-like modification modulates the partitioning of the Ran-GTPase-activating protein RanGAP1 between the cytosol and the nuclear pore complex. *J. Cell Biol.* **135**, 1457-1470.

Mo, Y. Y. and Moschos, S. J. (2005). Targeting Ubc9 for cancer therapy. *Expert Opin. Ther. Targets* **9**, 1203-1216.

Moschos, S. J. and Mo, Y. Y. (2006). Role of SUMO/Ubc9 in DNA damage repair and tumorigenesis. *J. Mol. Histol.* **37**, 309-319.

Mukhopadhyay, D. and Dasso, M. (2007). Modification in reverse: the SUMO proteases. *Trends Biochem. Sci.* **32**, 286-295.

Mukhopadhyay, D., Ayaydin, F., Kolli, N., Tan, S. H., Anan, T., Kametaka, A., Azuma, Y., Wilkinson, K. D. and Dasso, M. (2006). SUSP1 antagonizes formation of highly SUMO2/3-conjugated species. *J. Cell Biol.* **174**, 939-949.

Muller, S., Matunis, M. J. and Dejean, A. (1998). Conjugation with the ubiquitin-related modifier SUMO-1 regulates the partitioning of PML within the nucleus. *EMBO J.* **17**, 61-70.

Nacerddine, K., Lehembre, F., Bhaumik, M., Artus, J., Cohen-Tannoudji, M., Babinet, C., Pandolfi, P. P. and Dejean, A. (2005). The SUMO pathway is essential for nuclear integrity and chromosome segregation in mice. *Dev. Cell* **9**, 769-779.

Olivo-Marin, J.-C. (2002). Extraction of spots in biological images using multiscale products. *Pattern Recognit.* **35**, 1989-1996.

Parrinello, S., Samper, E., Krtolica, A., Goldstein, J., Melov, S. and Campisi, J. (2003). Oxygen sensitivity severely limits the replicative lifespan of murine fibroblasts. *Nat. Cell Biol.* **5**, 741-747.

Rosas-Acosta, G., Russell, W. K., Deyrieux, A., Russell, D. H. and Wilson, V. G. (2005). A universal strategy for proteomic studies of SUMO and other ubiquitin-like modifiers. *Mol. Cell Proteomics* **4**, 56-72.

Saitoh, H. and Hinchey, J. (2000). Functional heterogeneity of small ubiquitin-related protein modifiers SUMO-1 versus SUMO-2/3. *J. Biol. Chem.* **275**, 6252-6258.

Schatz, O., Golenser, E. and Ben-Arie, N. (2005). Clearing and photography of whole mount X-gal stained mouse embryos. *Biotechniques* **39**, 650, 652, 654 passim.

Seeler, J. S., Bischof, O., Nacerddine, K. and Dejean, A. (2007). SUMO, the three Rs and cancer. *Curr. Top. Microbiol. Immunol.* **313**, 49-71.

Shen, T. H., Lin, H. K., Scaglioni, P. P., Yung, T. M. and Pandolfi, P. P. (2006). The mechanisms of PML-nuclear body formation. *Mol. Cell* **24**, 331-339.

Sternsdorf, T., Jensen, K. and Will, H. (1997). Evidence for covalent modification of the nuclear dot-associated proteins PML and Sp100 by PIC1/SUMO-1. *J. Cell Biol.* **139**, 1621-1634.

Stryke, D., Kawamoto, M., Huang, C. C., Johns, S. J., King, L. A., Harper, C. A., Meng, E. C., Lee, R. E., Yee, A., L'Italien, L. et al. (2003). BayGenomics: a resource of insertional mutations in mouse embryonic stem cells. *Nucleic Acids Res.* **31**, 278-281.

Tatham, M. H., Jaffray, E., Vaughan, O. A., Desterro, J. M., Botting, C. H., Naismith, J. H. and Hay, R. T. (2001). Polymeric chains of SUMO-2 and SUMO-3 are conjugated to protein substrates by SAE1/SAE2 and Ubc9. *J. Biol. Chem.* **276**, 35368-35374.

Tatham, M. H., Kim, S., Jaffray, E., Song, J., Chen, Y. and Hay, R. T. (2005). Unique binding interactions among Ubc9, SUMO and RanBP2 reveal a mechanism for SUMO paralog selection. *Nat. Struct. Mol. Biol.* **12**, 67-74.

Tatham, M. H., Geoffroy, M. C., Shen, L., Plechanovova, A., Hattersley, N., Jaffray, E. G., Palvimo, J. J. and Hay, R. T. (2008). RNF4 is a poly-SUMO-specific E3 ubiquitin ligase required for arsenic-induced PML degradation. *Nat. Cell Biol.* **10**, 538-546.

Vertegaal, A. C., Ogg, S. C., Jaffray, E., Rodriguez, M. S., Hay, R. T., Andersen, J. S., Mann, M. and Lamond, A. I. (2004). A proteomic study of SUMO-2 target proteins. *J. Biol. Chem.* **279**, 33791-33798.

Vertegaal, A. C., Andersen, J. S., Ogg, S. C., Hay, R. T., Mann, M. and Lamond, A. I. (2006). Distinct and overlapping sets of SUMO-1 and SUMO-2 target proteins revealed by quantitative proteomics. *Mol. Cell Proteomics* **5**, 2298-2310.

Wu, F. and Mo, Y. Y. (2007). Ubiquitin-like protein modifications in prostate and breast cancer. *Front. Biosci.* **12**, 700-711.

Yamaguchi, T., Sharma, P., Athanasiou, M., Kumar, A., Yamada, S. and Kuehn, M. R. (2005). Mutation of SENP1/SuPr-2 reveals an essential role for desumoylation in mouse development. *Mol. Cell. Biol.* **25**, 5171-5182.

Zhang, X. D., Goeres, J., Zhang, H., Yen, T. J., Porter, A. C. and Matunis, M. J. (2008). SUMO-2/3 modification and binding regulate the association of CENP-E with kinetochores and progression through mitosis. *Mol. Cell* **29**, 729-741.